



DROPWISE CONDENSATION ON HYDROPHOBIC MICROPOROUS POWDER AND THE TRANSITION TO INTRAPOWDER DROPLET REMOVAL

Sean H. Hoenig^{1*}, Richard W. Bonner III¹

¹Advanced Cooling Technologies, Inc., Lancaster, PA 17601, USA

ABSTRACT

To improve condensation heat transfer technologies, various coating techniques have been used to generate rough hydrophobic surfaces. Condensation on micro-textured hydrophobic surfaces can demonstrate variable heat transfer enhancement compared to smooth hydrophobic surfaces. This is primarily directed towards the improvement in efficiency of condensers for direct dry cooling power plants. Here we investigate the use of a thiol-based self-assembled monolayer deposited on variably-sized microporous copper powder wick monolayers. A custom condensation chamber was fabricated to demonstrate the effect of enhanced dropwise condensation. Although rough hydrophobic surfaces have shown advantageous droplet growth dynamics, precise heat transfer measurements are underdeveloped at high heat flux. At consistent operating conditions, we experimentally demonstrated a 23% improvement in the local condensation heat transfer coefficient for a 4 μ m hydrophobic microporous copper powder surface compared to a smooth hydrophobic copper surface. This improvement is attributed to the reduction in contact angle hysteresis as evidenced by the decrease in departing droplet size. For larger powder sizes, surface flooding inhibited thermal performance due to larger departing droplet sizes and a decreased conduction pathway. With microporous powder sizes greater than 119 μ m, a transition of dropwise condensation to intrapowder droplet removal is evident. The use of enhanced two-phase thermal management technologies for high heat flux applications can benefit from the specific design of textured hydrophobic surfaces.

KEY WORDS: Dropwise condensation; Hydrophobicity; Microporous wick structures; Intrapowder droplet removal

1. INTRODUCTION

Dropwise condensation on textured non-wetting surfaces has vast applications in two-phase thermal management technologies, including power plant condensers, vapor chambers [1], and heat pipes. High heat transfer enhancement using dropwise condensation (DWC) has been of interest since the earliest published work in 1930, which reported an order of magnitude higher heat transfer coefficient compared to filmwise condensation for comparable conditions [2]. Although there are a multitude of different coating mechanisms to generate ultra-low surface energy, many issues remain to create a consistent, practical surface for industrial use. These issues include poor coating lifetime [3], constriction resistance for low thermally conductive materials [4], and high coating costs [5]. In spite of these issues, various hydrophobic micro/nano-textured structures have garnered close attention in recent years with respect to experimental research.

Several experimental studies have examined the supposed effects of micro/nano-textured structures to promote enhanced dropwise condensation. Dietz *et al.* [6] revealed the potential for greater heat transfer enhancement using textured superhydrophobic nanostructures due to the small size of departing droplets (< 10 μ m). Rykaczewski *et al.* [7, 8, 9, 10] demonstrated the need to use micro/nano surface features to confine droplet formation diameters to sub-10 μ m. During coalescence, larger diameter primary drops can actively contribute to sweeping smaller droplets to achieve higher departure rates. The nature of non-wetting states (Cassie or Wenzel) [11] on textured superhydrophobic surfaces also contributes to varying results. Narhe *et al.* [12, 13] determined there is a trade-off for textured surfaces between having high surface contact for a droplet in a

*Corresponding Author: Sean.Hoenig@1-ACT.com

Wenzel state or high mobility in a Cassie state for heat transfer efficiency. Two-tiered roughness structures [14] have additionally demonstrated sustained Cassie states for small droplet sizes.

In this study, the local condensation heat transfer coefficient is evaluated for hydrophobic microporous sintered copper powder structures, which extends the research of enhanced filmwise condensation using hydrophilic microporous sintered copper powder [15, 16]. This effort is to specifically quantify the extent of improvement in heat transfer efficiency for dropwise condensation on variably sized microporous copper wick monolayers and discuss the interface droplet effects of micro-textured hydrophobic surfaces. Microporous copper wick structures are widely used in heat pipe and vapor chamber designs [17] to transport condensate back to the evaporator section. Many studies regarding heat pipes have been completed to determine optimal performance using modulated wick structures for evaporation [18, 19, 20]. Additional research has examined the visual droplet morphology benefits of nanostructured wick substrates [21]. This is a continuation of the first comprehensive study to measure and understand the condensation heat transfer enhancement using hydrophobic microporous copper powder wick structures sintered on copper substrates.

2. EXPERIMENTAL

Test samples were machined out of commercially available copper alloy 101 to the specifications of the experimental setup. Figure 1 provides an in-depth look at the details of the experimental apparatus, which is oriented vertically. The active condensing surface is a 5.59cm x 2.03cm area centered in the test block. Figure 2 demonstrates the test blocks used for a smooth and textured surface as well as an example SEM image of the type of monolayer observed. The copper surfaces were first prepared using 1200 grit sandpaper to create a smooth finish and then cleaned with acetone. Microporous copper powder (ACuPowder) was then applied to the test surface to create a monolayer structure. This was done first through the application of a thin layer of Nicrobraz (Wall Colmonoy). The test blocks were then sintered to 975°C in a hydrogen furnace. The self-assembled monolayer was created using a 5mM solution of 1*H*,1*H*,2*H*,2*H*-perfluorodecanethiol (Sigma-Aldrich) dissolved in 2-propanol (Sigma-Aldrich). The test blocks were submerged in a sealed bath of the self-assembled monolayer solution for a 24-hour period and subsequently dried with dry nitrogen gas.

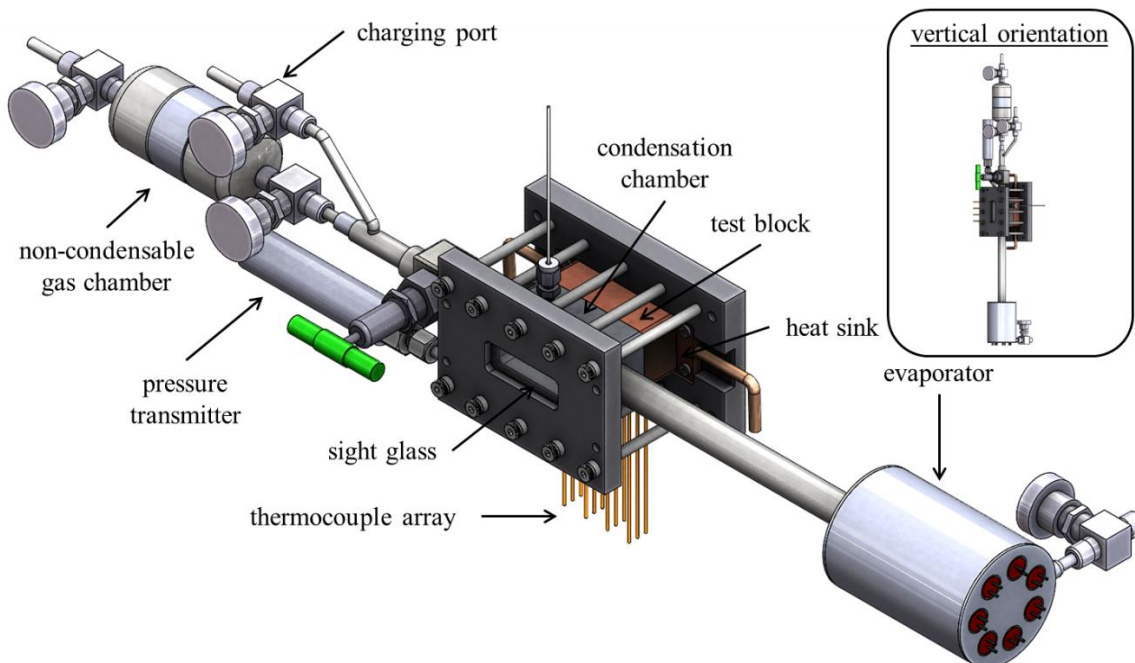


Fig. 1 The test setup demonstrated in SolidWorks in an isometric orientation. The actual orientation is vertical with the evaporator below the condensation chamber. The true orientation is represented in the inset image.

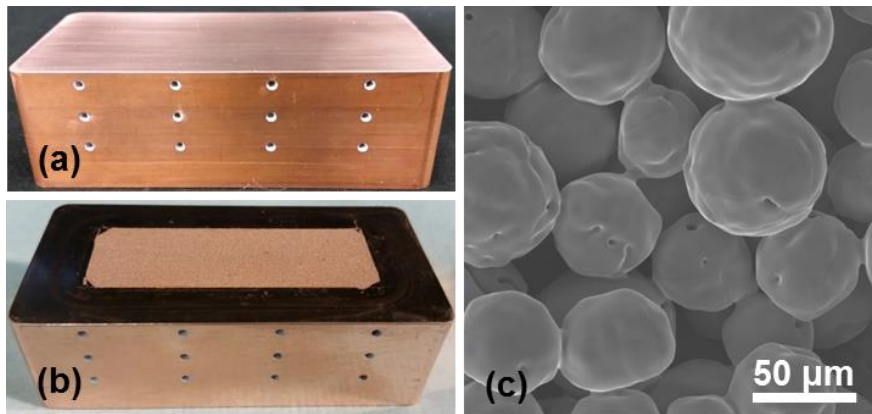


Fig. 2 A smooth copper surface (a) compared with a microporous copper powder wick sintered to a copper substrate (b). Image (c) is SEM for a $61\mu\text{m}$ diameter powder sample.

A graphic of the hydrophobic self-assembled monolayers deposited on a sintered microporous copper powder monolayer is shown in Figure 3. Each sample was then tested in the experimental apparatus using deionized water, which was injected following the use of a vacuum pump to evacuate the system. The absolute pressure for each experimental test was held between 222.49 to 244.69 kPa, which corresponds to a saturated vapor temperature of 105°C to 110°C . This pressure operating range was chosen to maintain a slightly higher saturated pressure than atmospheric conditions to prevent non-condensable gas (NCG) in-leak. During testing, the non-condensable gas (NCG) collection chamber was used to collect NCG and then purge the condensation chamber of any internal NCG buildup. To evaluate the surface temperature of the substrate for heat transfer calculations, a thermocouple array was used for interpolation. Thermal paste was used to ensure precise thermal coupling of the thermocouples to the thermocouple wells. Results were collected over a wide spectrum of heat flux data by varying the subsequent cartridge heater input and water chiller output. A transparent sight glass was incorporated to observe the dropwise condensation phenomenon.

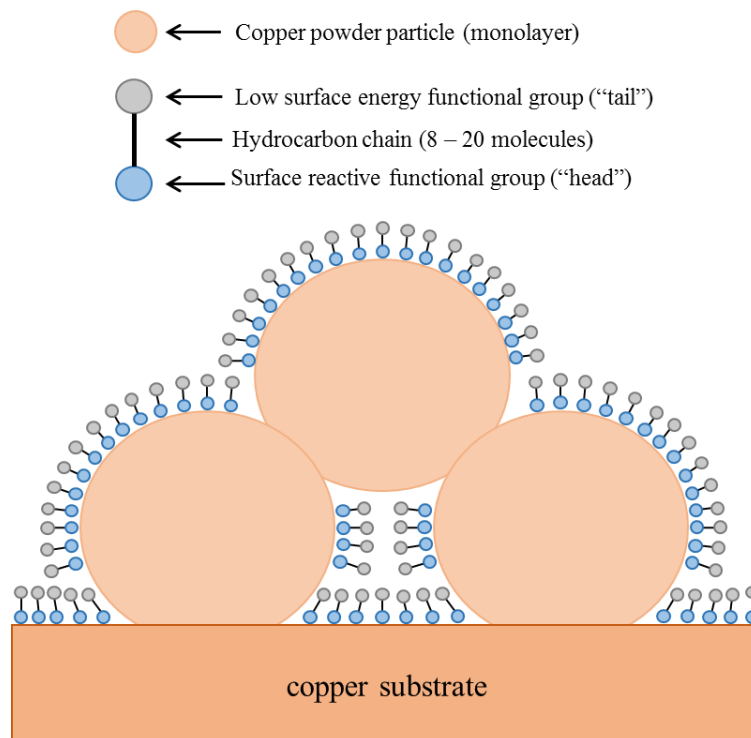


Fig. 3 Graphic of a self-assembled monolayer coating deposited on a sintered microporous copper powder monolayer and copper substrate.

Conduction calorimetry was used to calculate heat flux and extrapolate the surface temperature during dropwise condensation. Temperature measurements were acquired at several known locations within the copper test samples. Linear regression was then used to determine the thermal gradients across the block and extrapolate the surface temperature during dropwise condensation. Heat flux through the block was calculated using Fourier's Law, shown in Equation 1. The experimental dropwise condensation heat transfer coefficient was calculated using the measured saturated vapor temperature of the condensing steam and Newton's Law of Cooling, shown in Equation 2. A simplified expression for calculating the dropwise condensation heat transfer coefficient from these measurements is shown in Equation 3.

$$q'' = k_s \frac{dT}{dx} \quad (1)$$

$$q'' = h_l(T_v - T_s) \quad (2)$$

$$h_l = \frac{k_s \frac{dT}{dx}}{T_v - T_s} \quad (3)$$

3. SURFACE CHARACTERIZATION

An experimental trade study was performed where the particle size of microporous sintered copper powder was varied in order to evaluate their potential for heat transfer improvement in dropwise condensation. The different copper powders used are shown in Table 1, which additionally includes the apparent contact angles observed in air for sessile water droplets deposited on the surfaces. Visual representation of the apparent contact angle data are demonstrated in Figure 4. It is clear that the apparent contact angle for a smooth copper surface is only marginally hydrophobic at approximately 91°. As roughness is introduced on the copper surface in the form of increasingly larger copper powder monolayers, the apparent contact angle becomes superhydrophobic and greater than 140° for all samples except for the smallest powder size (4µm) and largest powder sizes (240µm, 416µm). The implication here is that the smallest microporous copper powder monolayer more closely emulates a smooth surface than the other roughness induced structures fabricated with larger sized powders. The largest powder sizes are an anomaly with the smaller apparent contact angle, which is evident with the thermal performance evaluation. The analytical importance of these observations becomes clearer as the heat transfer data are analyzed.

Table 1. Copper powder information for each sample tested. A minus sign “-” indicates that the powder passes through that screen mesh size while a plus sign “+” indicates that the powder is stopped by that screen mesh size. The apparent contact angle is indicative for each superhydrophobic microporous surface.

Powder Grade	Average Powder Diameter (µm)	θ _a (degrees)
Smooth	None	91.0±0.6°
2000	4 µm	127.5±2.2°
500A (-325)	21 µm	140.8±2.0°
155A (-325)	43 µm	153.5±1.5°
103A (-150/+325)	61 µm	153.5±1.0°
Cu31 (-80/+150)	119 µm	141.8±0.8°
68HP (-50/+60)	240 µm	133.0±1.3°
34HP (-30/+40)	416 µm	131.5±1.7°

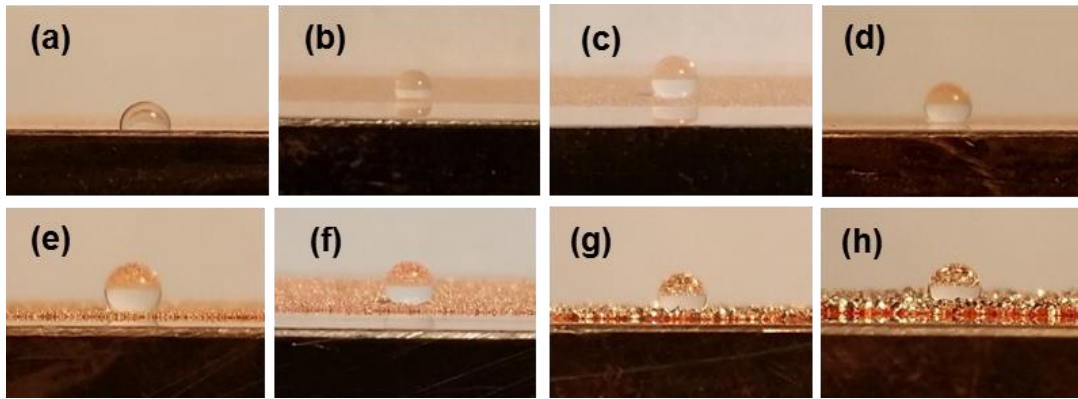


Fig. 4 Water droplets approximately 10.12 μ L deposited on superhydrophobic microporous copper powder. The average powder diameter used for each sample is (a) none, (b) 4 μ m, (c) 21 μ m, (d) 43 μ m, (e) 61 μ m, (f) 119 μ m, (g) 240 μ m, and (h) 416 μ m.

4. THERMAL PERFORMANCE EVALUATION

All measured heat transfer results from this effort are found in Figure 5, which shows the local vapor-to-surface temperature difference (ΔT) as a function of the local condensation heat flux (q''). The results for a smooth hydrophobic copper surface ($h_1 = 156 \pm 3 \text{ kW/m}^2\text{-K}$) represent a baseline comparison for thermal performance. The plot of experimental data for ΔT versus heat flux for the different powder and smooth surfaces show a generally linear trend, indicating a constant heat transfer coefficient as a function of heat flux. This allows the data to be represented well as a single heat transfer coefficient measurement (using the slope of the regression line) for each type of surface, shown in Figure 6. In this figure, the data are more clearly represented to demonstrate the local condensation heat transfer coefficient as a function of average powder diameter. With a consistently sized monolayer powder surface, this graphical representation demonstrates the trend in thermal performance for surface roughness from the smallest powder size to the largest powder size. A 23% improvement in the local heat transfer coefficient ($h_1 = 183 \pm 6 \text{ kW/m}^2\text{-K}$) is evident for the smallest copper powder size (4 μ m) compared to a smooth surface. The droplet growth for the 4 μ m powder sample is likely in the partially-wetting mode for a Cassie-state droplet [22]. The partially-wetting mode droplet morphology enhances the heat transfer efficiency for Cassie-state droplets due to the ability for vapor to penetrate beneath the wick structure and directly condense within the wick [23]. To extend the findings of Miljkovic *et al.*, the liquid bridge formed between the copper surface and the droplet growing along the microporous powder is relatively high in thermal conductivity. If this liquid bridge exists, this parallel conduction heat transfer path likely contributes to the enhanced thermal performance observed for the 4 μ m powder sample. Additional surface imaging during condensation using ESEM would demonstrate the true nature of this phenomenon.

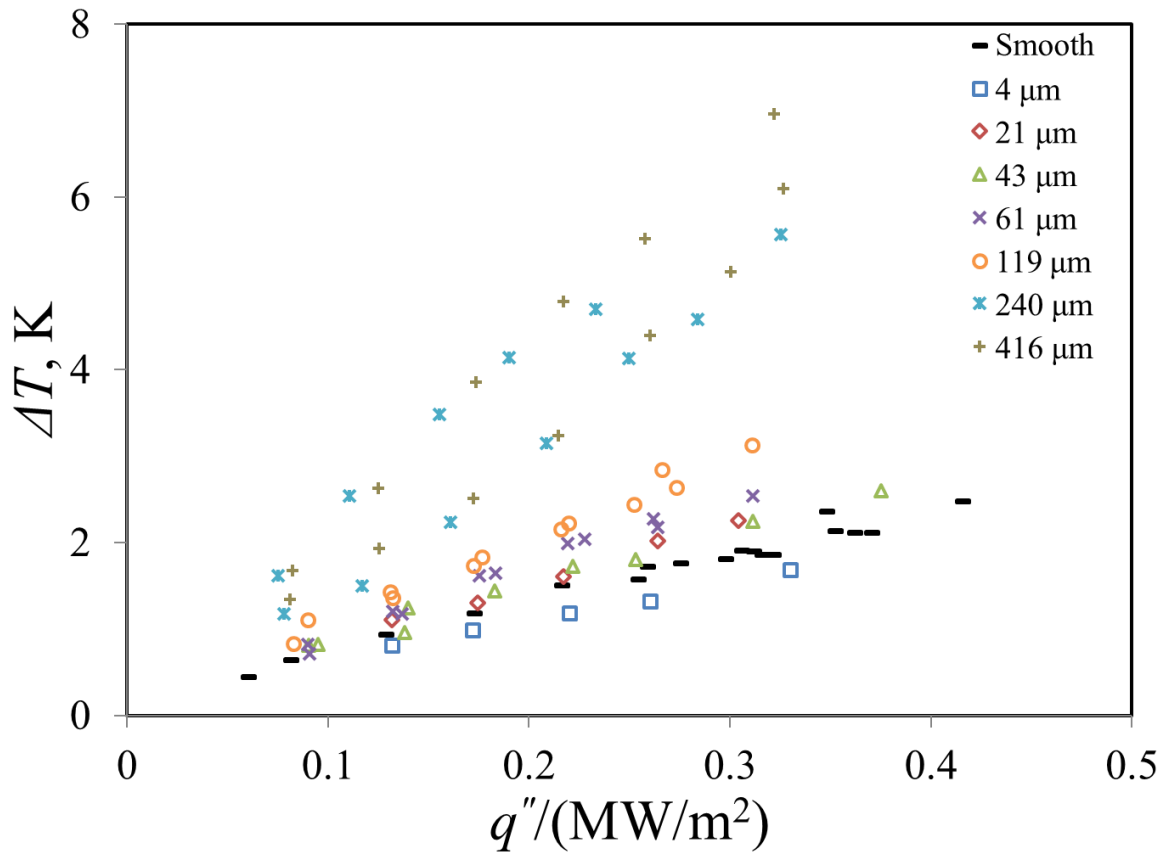


Fig. 5 The local vapor-to-surface temperature difference plotted against the local condensation heat flux is used to analyze the heat transfer efficiency of the superhydrophobic microporous wick structures.

The subsequent data for larger powder sizes are progressively worse in thermal performance. This is due to the formation of more highly pinned droplets with high contact angle hysteresis and droplet growth in a mixed wettability mode on the wick structures [12, 24]. The increased hysteresis increases the maximum departing droplet size, creating a shift in droplet size distribution towards larger droplets. Evidence of this pinning effect can be seen in Figure 7 for larger copper powder sizes. The increased average droplet size increases the conduction resistance, leading to decreased heat transfer efficiency. The thermal performance is also worse due to the exhibited mixed wettability mode that is demonstrated by these larger powder size (43 μm and greater) wicked substrates. In this mixed wettability mode, condensation can occur on the liquid film near the top of the wick structure, rather than exclusively within the powder layer as demonstrated with the smaller diameter powders operating in a partially-wetted mode [25]. This would lead to an increased liquid conduction resistance in a suspended wetting mode as compared to the case where droplet growth occurs directly at the base of the wick structure. The results additionally suggest that another transition begins to occur for a larger powder sample (119 μm diameter). It is clear that the liquid condensing within the wick structure does not collect in the droplets above the wick, but travel as a film beneath the wick [26, 27]. The results indicate that this more extreme transition to decreased thermal performance is evident for the largest powder sizes (240 μm , 416 μm). For these samples, the increased film thickness beneath the wick structure contributes to a severely worse thermal performance than a smooth hydrophobic surface. The large diameter copper powder particles are too widely separated to generate small departing droplets with low hysteresis, which prevents the consistent formation of droplets. Amorphous droplets with high hysteresis combined with thin films form on and within the powder layer. With the apparent condensation beneath the powder surface, the large conduction resistance ensures low efficiency for large microporous powder surfaces. It would be more appropriate to define this phenomenon as “intrapowder droplet removal” due to the surface flooding and subsequent removal of condensed droplets beneath the microporous wick structure.

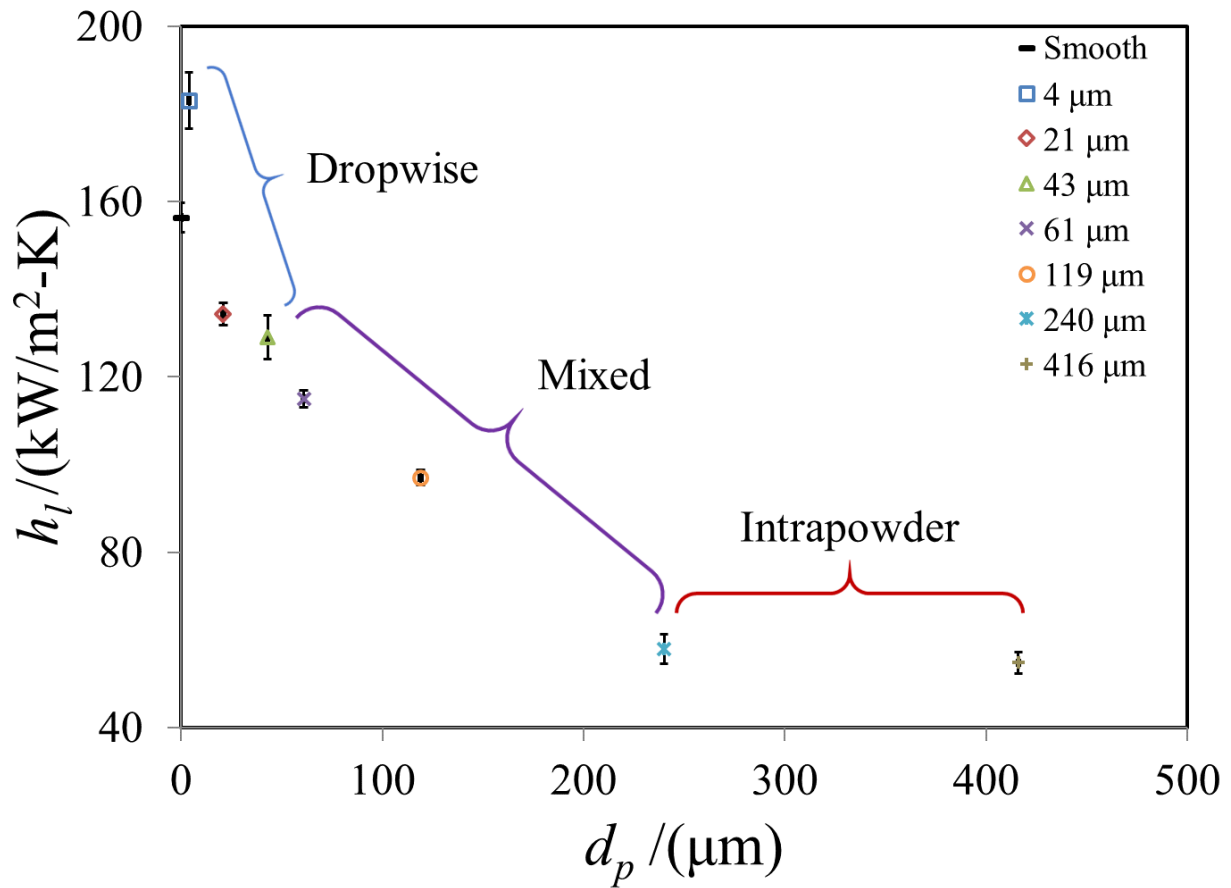


Fig. 6 The heat flux averaged local heat transfer coefficient plotted against copper powder diameter to demonstrate the trend in thermal performance from smallest to largest powder size. The smallest hydrophobic copper powder (4 μm) surface outperforms a smooth hydrophobic surface by 23%. The largest hydrophobic copper powders (>119 μm) exhibit intrapowder droplet removal, which leads to decreased thermal performance.

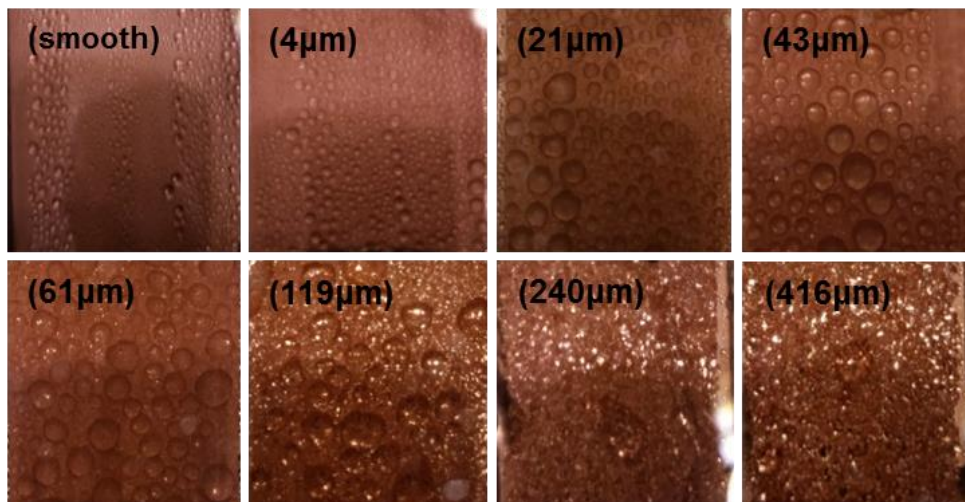


Fig. 7 Droplet growth for a smooth, 4 μm , 21 μm , 43 μm , 61 μm , 119 μm , 240 μm , and 416 μm copper powder surface. Highly pinned amorphous droplets with high hysteresis contribute to decreased heat transfer efficiency for larger powder sizes. Small departing droplets with low hysteresis contribute to increased heat transfer efficiency for the smallest powder size.

5. DEPARTING DROPLET SIZE

The high heat transfer efficiency of the smallest copper powder size (4 μm) compared to a smooth copper surface is a significant distinction. Without including the results of the 4 μm powder, the smooth hydrophobic copper surface demonstrates the highest heat transfer coefficients. The relatively high heat transfer coefficients with the smooth surface are attributed to its relatively low contact angle hysteresis and zero additional conduction resistance. Further observations show that the departing droplet size appears to be the primary variable governing heat transfer, in addition to secondary explanations, such as the droplet growth mode, conduction resistance, and filmwise modes of condensation underneath the powder structures. These findings are in reference to [28], which the subsequent departing droplet size observations are exclusively based on. In this complementary study by Hoenig *et al.*, the maximum departing droplet sizes were measured for several departing droplets located near the top of all of the condensation surfaces. This does not include the largest microporous surfaces (240 μm , 416 μm), as discernable droplets were not demonstrated for these samples. The measurements were acquired using burst shot imaging of the droplets at consistent high heat flux and measuring the droplet sizes digitally immediately before droplet departure. Empirical photo evidence used is comparable to what is shown above in Figure 7. The results of these measurements are plotted in Figure 8, which shows the thermal performance data as a function of maximum departing droplet radii. A clear trend of decreasing heat transfer with increasing departing droplet size is evident, regardless of whether or not the surface is smooth or modified with sintered powder. A power law relationship exists for the local heat transfer coefficient as a function of departing droplet radius across all surfaces, both smooth and textured, with a value of -0.57 . Here it is noted that this is consistent with the model developed and correlated by Bonner [29], which indicated a power law relationship value between $-1/2$ and $-2/3$ for the heat transfer efficiency of the condensation of steam as a function of departing droplet radius.

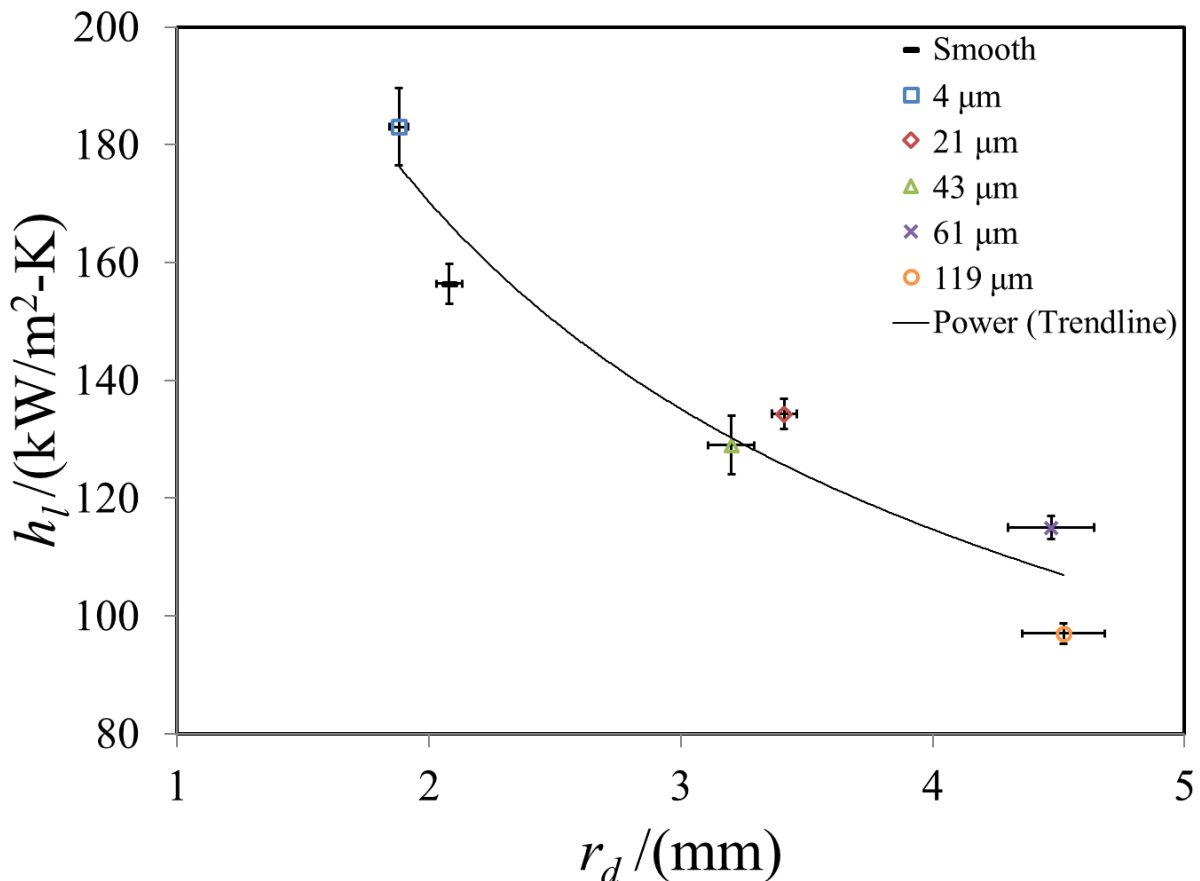


Fig. 8 The heat flux averaged local heat transfer coefficient plotted against maximum departing droplet radius for each surface. This evidence demonstrates why the smallest hydrophobic copper powder (4 μm) surface demonstrates better thermal performance than

a smooth hydrophobic copper surface. The small departing droplet radii with low hysteresis are efficiently removed from the surface. A power law relationship exists for the data with a value of -0.574 . This is consistent with the findings from the Bonner correlation [29], which indicated a power law relationship value between $-1/2$ and $-2/3$ for the condensation of steam. The trendline equation is: $h_l = 253r_d^{-0.57}$.

6. CONCLUSION

Hydrophobic surfaces were developed using self-assembled monolayers deposited on microporous copper powder wick structures, which are commonly and cost effectively used in heat pipe manufacturing. The local heat transfer coefficient for dropwise condensation of steam on these surfaces was then experimentally measured. As a result, local heat transfer coefficients for the larger powder surfaces ($21\mu\text{m}$ diameter and greater) were lower than local heat transfer coefficients obtained on a smooth copper surface. Competing factors influence the decreased thermal efficiency observed. The formation of strongly pinned droplets led to a shift in the departing droplet size distribution towards larger sizes. The large departing droplet radii and secondarily additional conduction resistance both contributed to decreased thermal performance. The smallest microporous copper powder structure ($4\mu\text{m}$) demonstrated a 23% improvement in the local heat transfer coefficient compared to a smooth copper surface. The partially-wetting droplet growth mode for the $4\mu\text{m}$ powder sample, as opposed to the mixed wettability mode, contributed to enhanced heat transfer efficiency. The largest microporous copper powder structures ($240\mu\text{m}$, $416\mu\text{m}$) exhibited an intrapowder droplet removal that demonstrated a 65% degradation in the local heat transfer coefficient compared to a smooth copper surface. With large sintered copper powder particles, inconsistent droplet formation led to an increased liquid film thickness formed within the wick structure. A clear trend was identified where heat transfer coefficients correlated strongly with the maximum departing droplet size for both smooth and sintered powder coated surfaces. The correlation between heat transfer and departing droplet size that was identified is also consistent with other correlations developed for multiple fluids on smooth surfaces. The design of hydrophobic porous surfaces could lead to more efficient two-phase thermal management at high heat flux if the appropriate wetting mode under saturated steam conditions can be realized.

ACKNOWLEDGMENT

This work was funded by the Office of Science in the U.S. Department of Energy (DOE) under a Phase II SBIR grant, award number DE-SC-0011317. The program manager was Robie Lewis. The authors would like to thank Phil Martin and Maksym Demydovych for their testing expertise, as well as Professor Massoud Kaviany and Minki Kim from the University of Michigan for the sample SEM images.

NOMENCLATURE

q''	Heat flux through condensing surface	(MW/m ²)	T_s	Surface temperature	(°C)
h_l	Local heat transfer coefficient	(kW/m ² -K)	ΔT	Vapor and surface temperature difference	(°C)
k_s	Substrate thermal conductivity	(W/m-K)	$\frac{dT}{dx}$	Temperature gradient with respect to path length	(°C/m)
χ	Path length through test block	(m)	d_p	Average copper powder diameter	(μm)
T_v	Vapor temperature at saturation pressure	(°C)	r_d	Maximum departing droplet radius	(mm)

REFERENCES

- [1] R. W. Bonner III, "Dropwise Condensation in Vapor Chambers," in *IEEE SEMI-THERM*, Santa Clara, CA, 2010.
- [2] E. Schmidt, W. Schurig and W. Sellschopp, "Versuche uber die Kondensation in Film- und Tropfenform," *Tech. Mech. Thermodynamik*, vol. 1, pp. 55-63, 1930.
- [3] R. Bonner III, "Dropwise Condensation Life Testing of Self-Assembled Monolayers," in *Proceedings of the International Heat Transfer Conference, IHCT 14*, Washington, D.C., 2011.
- [4] J. Rose, "Dropwise condensation theory and experiment: A review," *Proc. Inst. Mech. Eng. Part A: J. Power Energy*, vol. 216, pp. 115-128, 2002.
- [5] R. W. Bonner III, "Dropwise Condensation on Surfaces with Graded Hydrophobicity," in *ASME Summer Heat Transfer Conference*, San Francisco, CA, 2009.
- [6] C. Dietz, K. Rykaczewski, A. G. Fedorov and Y. Joshi, "Visualizations of Droplet Departure on a Superhydrophobic Surface and Implications to Heat Transfer Enhancement during Dropwise Condensation," *Applied Physics Letters*, vol. 97, p. 033104, 2010.
- [7] K. Rykaczewski, W. A. Osborn, J. Chinn, M. L. Walker, J. H. J. Scott, W. Jones, C. Hao, S. Yao and Z. Wang, "How Nanorough is Rough Enough to Make a Surface Superhydrophobic during Water Condensation?," *Soft Matter*, vol. 8, p. 8786, 2012.
- [8] K. Rykaczewski, J. H. J. Scott, S. Rajauria, J. Chinn, A. M. Chinn and W. Jones, "Three Dimensional Aspects of Droplet Coalescence during Dropwise Conensation on Superhydrophobic Surfaces," *Soft Matter*, vol. 7, p. 8749, 2011.
- [9] K. Rykaczewski, A. T. Paxson, S. Anand, X. Chen, Z. Wang and K. K. Varanasi, "Multimode Multidrop Serial Coalescence Effects during Condensation on Hierarchical Superhydrophobic Surfaces," *Langmuir*, vol. 29, pp. 881-891, 2013.
- [10] K. Rykaczewski, "Microdroplet Growth Mechanism during Water Condensation on Superhydrophobic Surfaces," *Langmuir*, vol. 28, pp. 7720-7729, 2012.
- [11] B. He, N. A. Patankar and J. Lee, "Multiple Equilibrium Droplet Shapes and Design Criterion for Rough Hydrophobic Surfaces," *Langmuir*, vol. 19, pp. 4999-5003, 2003.
- [12] R. D. Narhe and D. A. Beysens, "Growth Dynamics of Water Drops on a Square-Pattern Rough Hydrophobic Surface," *Langmuir*, vol. 23, pp. 6486-6489, 2007.
- [13] R. D. Narhe and D. A. Beysens, "Nucleation and Growth on a Superhydrophobic Grooved Surface," *Physical Review Letters*, vol. 93, no. 7, p. 076103, 2004.
- [14] C.-H. Chen, Q. Cai, C. Tsai, C.-L. Chen, G. Xiong, Y. Yu and Z. Ren, "Dropwise Condensation on Superhydrophobic Surfaces with Two-tier Roughness," *Applied Physics Letters*, vol. 90, p. 173108, 2007.
- [15] Y. Zheng, C.-H. Chen, H. Pearlman, M. Flannery and R. Bonner, "Effect of Porous Coating on Condensation Heat Transfer," Boulder, Colorado, 2015.
- [16] Y. Zheng, C.-H. Chen, H. Pearlman and R. Bonner, "Enhanced Filmwise Condensation with Thin Porous Coating," Hawaii's Big Island, 2016.
- [17] A. Faghri, *Heat Pipe Science and Technology*, Washington, D.C.: Taylor & Francis, 1995.
- [18] G. S. Hwang, M. Kaviany, W. G. Anderson and J. Zuo, "Modulated wick heat pipe," *International Journal of Heat and Mass Transfer*, vol. 50, pp. 1420-1434, 2007.
- [19] G. S. Hwang, E. Fleming, B. Carne, S. Sharratt, Y. Nam, P. Dussinger, Y. S. Ju and M. Kaviany, "Multi-artery heat-pipe spreader: Lateral liquid supply," *International Journal of Heat and Mass Transfer*, vol. 54, pp. 2334-2340, 2011.
- [20] G. S. Hwang, Y. Nam, E. Fleming, P. Dussinger, Y. S. Ju and M. Kaviany, "Multi-artery heat pipe spreader: Experiment," *International Journal of Heat and Mass Transfer*, vol. 53, pp. 2662-2669, 2010.

- [21] D. M. Anderson, M. K. Gupta, A. A. Voevodin, C. N. Hunter, S. A. Putnam, V. V. Tsukruk and A. G. Fedorov, "Using Amphiphilic Nanostructures To Enable Long-Range Ensemble Coalescence and Surface Rejuvenation in Dropwise Condensation," *ACS Nano*, vol. 6, no. 4, pp. 3262-3268, 2012.
- [22] H. J. Cho, D. J. Preston, Y. Zhu and E. N. Wang, "Nanoengineered materials for liquid-vapour phase-change heat transfer," *Nature Reviews - Materials*, vol. 2, no. 16092, 2016.
- [23] N. Miljkovic, R. Enright and E. N. Wang, "Effect of Droplet Morphology on Growth Dynamics and Heat Transfer during Condensation on Superhydrophobic Nanostructured Surfaces," *ACS Nano*, vol. 6, no. 2, pp. 1776-1785, 2012.
- [24] N. Miljkovic, R. Enright, Y. Nam, K. Lopez, N. Dou, J. Sack and E. N. Wang, "Jumping-Droplet-Enhanced Condensation on Scalable Superhydrophobic Nanostructured Surfaces," *Nano Letters*, vol. 13, pp. 179-187, 2013.
- [25] N. Miljkovic, R. Enright and E. N. Wang, "Condensation Heat Transfer on Superhydrophobic Surfaces," *MRS Bull*, vol. 38, pp. 397-406, 2013.
- [26] K. A. Wier and T. J. McCarthy, "Condensation on Ultrahydrophobic Surfaces and its Effect on Droplet Mobility: Ultrahydrophobic Surfaces are not Always Water Repellant," *Langmuir*, vol. 22, pp. 2433-2436, 2006.
- [27] J. Cheng, A. Vandadi and C.-L. Chen, "Condensation Heat Transfer on Two-tier Superhydrophobic Surfaces," *Applied Physics Letters*, vol. 101, p. 131909, 2012.
- [28] S. H. Hoenig and R. W. Bonner III, "Dropwise Condensation on Superhydrophobic Microporous Wick Structures," *Journal of Heat Transfer*, Accepted, 2017.
- [29] R. W. Bonner III, "Correlation for dropwise condensation heat transfer: Water, organic fluids, and inclination," *International Journal of Heat and Mass Transfer*, vol. 61, pp. 245-253, 2013.